# Cholinergic-associated loss of hnRNP-A/B in Alzheimer's disease impairs cortical splicing and cognitive function in mice

*Amit Berson[1], Shahar Barbash[1], Galit Shaltiel[1], Yael Goll[1], Geula Hanin[1], David S. Greenberg[1], Maya Ketzef[2], Albert J Becker[3], Alon Friedman[2], Hermona Soreq[1]**

Keywords: alternative splicing; Alzheimer's disease; cholinergic signalling; hnRNP; RNA

DOI 10.1002/emmm.201100995

Received October 07, 2011
Revised April 05, 2012
Accepted April 12, 2012

Genetic studies link inherited errors in RNA metabolism to familial neurodegenerative disease. Here, we report such errors and the underlying mechanism in sporadic Alzheimer's disease (AD). AD entorhinal cortices presented globally impaired exon exclusions and selective loss of the hnRNP A/B splicing factors. Supporting functional relevance, hnRNP A/B knockdown induced alternative splicing impairments and dendrite loss in primary neurons, and memory and electrocorticographic impairments in mice. Transgenic mice with disease-associated mutations in APP or Tau displayed no alterations in hnRNP A/B suggesting that its loss in AD is independent of Aβ and Tau toxicity. However, cholinergic excitation increased hnRNP A/B levels while *in vivo* neurotoxin-mediated destruction of cholinergic neurons caused cortical AD-like decrease in hnRNP A/B and recapitulated the alternative splicing pattern of AD patients. Our findings present cholinergic-mediated hnRNP A/B loss and impaired RNA metabolism as important mechanisms involved in AD.

## INTRODUCTION

AD is the leading cause of dementia, accounting for 50–80% of dementia cases and afflicting 35 million worldwide. The vast majority of patients are defined as sporadic (Querfurth & LaFerla, 2010), but none of the currently recognized causes of AD can fully explain the disease phenotype. For example 40% of amyloid plaque pathology carriers do not develop AD (Ashe & Zahs, 2010) and amyloid-independent mechanisms have been recently acknowledged (Pimplikar et al, 2010). At another level, roughly 50% of known debilitating mutations in RNA-binding proteins cause neuronal-related diseases (Cooper et al, 2009; Licatalosi & Darnell, 2006), and several neuron-specific splicing factors (e.g. NOVA) regulate distinct transcript sets critical for proper neuronal functions (Zhang et al, 2010). Further corroborating the link between RNA splicing and neuronal survival, mutations in the SMN2 gene induce spliceosome mis-assembly and motor neuron degeneration in spinal muscular atrophy (Lefebvre et al, 1995; Zhang et al, 2008), and mutations in the RNA-binding proteins TDP-43 and FUS induce amyotrophic lateral sclerosis (Kabashi et al, 2008; Sreedharan et al, 2008; Vance et al, 2009). In several engineered mouse models of human degenerative diseases, transcriptome profiling demonstrated alternative splicing perturbations (Du et al, 2010; Zhang et al, 2008), suggesting that global changes in the repertoire of mRNA variants may be involved in the initiation and/or progression of these diseases. However, whether splicing impairments may also be involved in sporadic, non-familial neurodegeneration has not been studied.

Of particular relevance are members of the heterogeneous nuclear ribonucleoproteins hnRNP A/B family, namely hnRNP A1 and A2/B1 which are among the most abundant nuclear proteins. The modular structure of hnRNPs A/B contains several RNA binding motifs spanning RNA recognition motifs (RRM) and arginine-glycine-glycine (RGG) boxes. Several lines of

(1) Department of Biological Chemistry and the Edmond and Lily Safra Center of Brain Science, The Hebrew University of Jerusalem, Jerusalem, Israel
(2) Department of Physiology, Zlotowski Center for Neuroscience, Ben-Gurion University of the Negev, Beer-Sheva, Israel
(3) Department of Neuropathology, University of Bonn Medical Center, Bonn, Germany
***Corresponding author:** Tel: +972 2 658 5109; Fax: +972 2 652 0258; E-mail: soreq@cc.huji.ac.il

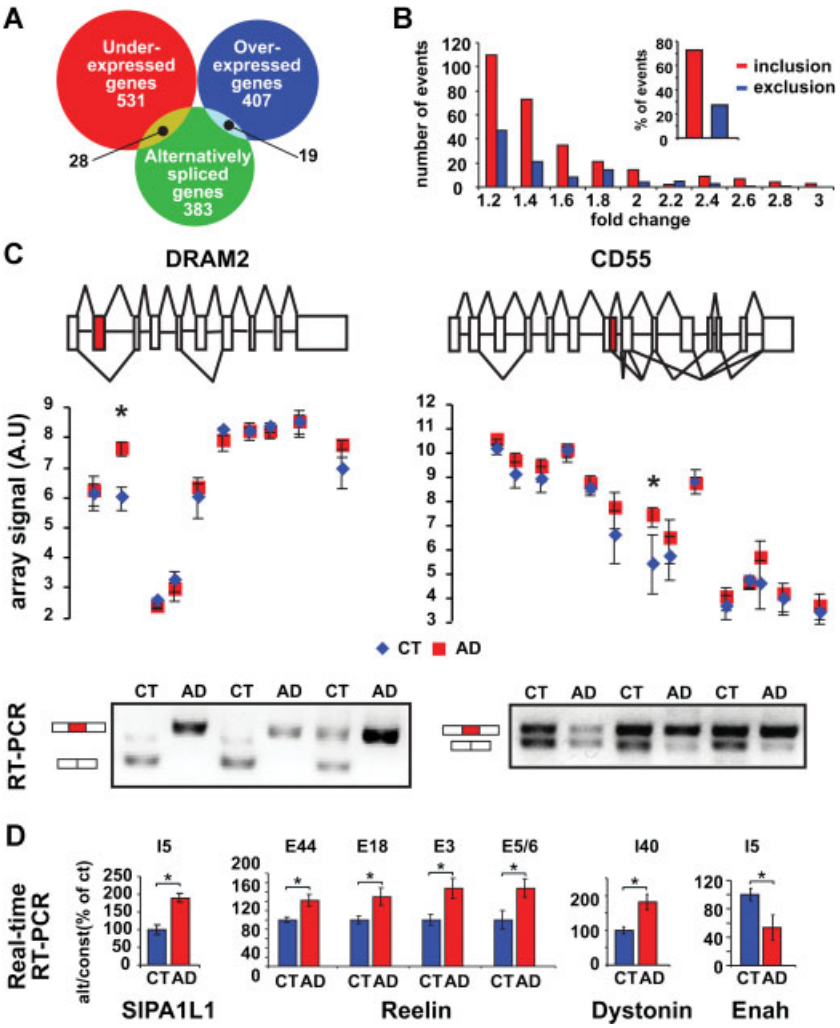


**Figure 1. Global alternative splicing alterations in the entorhinal cortex of AD patients.**

**A.** Venn diagram of gene expression and alternative splicing changes between AD patients and non-demented controls.

**B.** The majority of splicing events in AD involved exon inclusions. Kolmogorov–Smirnov test: $p < 0.0001$.

**C.** Two examples of gene structure (top), array expression levels of individual exons in AD and controls (middle), and RT-PCR validations (bottom) for DRAM2 and CD55.

**D.** Real-time RT-PCR validations of alternative splicing events in SIPA1L1, Reelin, Dystonin and Enah. $^{*}p < 0.05$, Student's *t*-test, $n = 7$ for both groups. Alternative exon levels are normalized to a constitutive exon from the same gene.

evidence suggest critical roles for hnRNP A/B proteins in neurons. Specifically, hnRNP A1 represses SMN2 exon 7 splicing (Kashima et al, 2007), and hnRNP A1 polymorphisms have been linked to frontotemporal lobar degeneration (FTLD; Villa et al, 2011). Recently, hnRNP A1 expression was shown to be increased in peripheral blood mononuclear cells from AD patients (Villa et al, 2011). Also, autoantibodies against hnRNP A1 have been identified in human T-lymphotropic virus type 1 (HTLV-1)-associated myelopathy/tropical spastic paraparesis (HAM/TSP), a disease that can be indistinguishable from multiple sclerosis (MS; Levin et al, 2002). Importantly, these autoantibodies stained neurons and inhibited neuronal firing in brain slices (Levin et al, 2002). Based on these reports, we hypothesized that regulation of RNA metabolism, and specifically hnRNP A/B-mediated alternative splicing might be especially important in the context of non-familial neurodegeneration.

Here, we show global aberrant splicing in AD entorhinal cortices, which is accompanied by selective reduction in the levels of hnRNP A/B proteins. Suppression of individual or combined hnRNP A/B induced dendrite and synapse loss, altered electrocorticographic (ECoG) patterns and caused severe learning and memory impairments. Surprisingly, primary cortical neurons, transgenic mice and stereotactic brain injections all indicated that hnRNP A/B reduction is Aβ and Tau independent; rather, we found that acetylcholine signalling, which is drastically reduced in AD, is a major regulator of hnRNP A/B expression and alternative splicing, *in vivo*.

## RESULTS

For initiating an unbiased search for transcriptional changes in AD, we applied exon-level microarray analysis on postmortem entorhinal cortices from AD patients and age-matched non-demented controls. To gain focused information on alternative splicing, we calculated the expression level for each known exon in the human transcriptome relative to the expression of the entire gene, and sub-classified transcripts into those whose general levels or only alternative splicing patterns were modified, thus gaining access to previously unexplored AD-related transcript changes. 531 and 407 genes were under- or over-expressed by more than twofold in AD samples, respectively (Fig 1A). These predictably belong to multiple gene

  

ontology (GO) categories related to synaptic transmission (Supporting Information Fig S1). Synaptic deficits are well known to be characteristic of AD (Armstrong et al, 1991), which corroborates our analysis. In comparison, we identified 383 exons whose ratio of exon inclusion is significantly different between the AD and control groups. These exons belong to 319 genes whose general level of expression was not changed significantly, and thus in most cases a single exon was differently spliced in each gene. GO analysis revealed that these alternatively spliced transcripts belong to categories such as regulation of ubiquitin protein-ligase activity (Tai & Schuman, 2008), isomerase activity (Pastorino et al, 2006; Uehara et al, 2006), neuron projections (Luo & O'Leary, 2005) and RNA-binding activity (Supporting Information Fig S1; Cooper et al, 2009; Licatalosi & Darnell, 2006). Thus, splicing and transcription modifications both affect large gene groups of neurodegeneration-relevant categories.

Of note, 75% of the AD-alternatively spliced exons demonstrated increased inclusion, predicting selective changes in splicing regulators (Fig 1B). In seven human entorhinal cortex samples in each group, reverse transcribed polymerase chain reaction (RT-PCR) and real-time RT-PCR, validated AD-associated alternative splicing in transcripts involved in dendritic spine morphology (SIPA1L1; Pak et al, 2001), synaptic plasticity (Reelin; Kocherhans et al, 2010), neurodegeneration (Dystonin; Sonnenberg & Liem, 2007), neuronal response to injury (CD55; Wang et al, 2010) and cell death (DRAM2; Park et al, 2009; Fig 1C and D).

To explore the molecular origin of the observed changes, we analysed protein and mRNA levels of several splicing factors and spliceosomal components in the entorhinal cortex of AD patients and controls. In splice site selection, SR proteins bind to splicing enhancer elements, whereas hnRNPs mostly bind to silencer elements (Mayeda & Krainer, 1992), inversely inhibiting the splicing reaction (Chen & Manley, 2009). We observed no changes in SR protein levels (Fig 2A), the SR kinases SRPK1 and SRPK2 or small nuclear RNA (U1, U2, U11 and U12; Supporting Information Fig S1). In contrast, hnRNP A/B proteins were almost completely absent in entorhinal cortices from AD patients, contrasting the robust nuclear staining of control tissues (Fig 2A). *In silico* analysis identified potential high affinity hnRNP binding sites (Burd & Dreyfuss, 1994) at or near all of the validated alternative splicing events. hnRNP A/B proteins are ubiquitously expressed but show higher expression in neurons than in glia (Kamma et al, 1995). To gain insight into the relationship between AD pathology and loss of hnRNP A/B expression, we triple labelled the human entorhinal cortex with antibodies against hnRNP A/B or SR proteins, a thioflavin-S staining which marks plaques and tangles and DNA counter staining to visualize intact nuclei. These staining reactions demonstrated that SR proteins are maintained even in neurons with massive tangle morphology (Fig 2B), and validated the almost complete loss of hnRNP A/B in all observed nuclei, including those of tangle-bearing neurons. Further, this analysis showed that expression of both hnRNP A/B and SR proteins is more prominent in neuronal nuclei but only hnRNP A/B are reduced in AD, arguing against a simple loss of neurons as the underlying mechanism. Finally, we tested the disease specificity of this phenomenon by analysing hnRNP A/B expression in sclerotic hippocampal samples removed at surgery from patients with chronic pharmaco-resistant temporal lobe epilepsy who underwent surgical treatment in the Epilepsy Surgery Program at the University of Bonn Medical Center. These samples showed high expression of hnRNP A/B (Fig 2C), demonstrating no loss of hnRNP A/B in temporal lobe epilepsy.

To challenge these findings using a different method, we employed immunoblotting of homogenates made from entorhinal cortex samples of AD patients and controls, using SR-targeted antibodies, a pan-hnRNP A/B monoclonal antibody and antibodies selective for A1 and A2/B1. This analysis validated the loss of hnRNP A/B proteins in patients with advanced Braak pathology (stages 5–6; Fig 3A) while showing no significant difference in non-demented patients with Braak's stages of 3–4 (Fig 3A and Supporting Information Fig S2), and supported the findings of sustained levels of SR proteins in AD tissues (Fig 3B). To test hnRNP A/B levels in another neurodegenerative disease, we analysed postmortem *substantia nigra pars compacta* samples from Parkinson's disease (PD) patients and found no reduction, and even a slight increase in hnRNP A/B levels compared to controls (Supporting Information Fig S1). Nevertheless, cholinergic impairments increase the risk of Parkinsonism in humans and mice alike: we have recently shown that over-expression of the 'synaptic' AChE-S variant exacerbates MPTP sensitivity, whereas enforced excess of the soluble AChE-R splice variant exerts neuroprotection from MPTP (Benmoyal-Segal et al, 2012; Soreq et al, 2012). To gain new insights into the potential role of hnRNPs in the cholinergic contribution to Parkinsonism, we tested hippocampal RNA preparations from the brain of engineered model mice. In line with our current study, RT-PCR tests showed considerably higher levels of hnRNP A1, A2/B1 and A3 in the hippocampi from the protected TgR over-expressors of AChE-R as compared to the vulnerable TgS over-expressors of AChE-S (Supporting Information Fig S3). Thus, hnRNPs appear not to be grossly depleted from the Parkinsonian brain, but are induced by the cholinergic reaction to dopaminergic poisons.

A central question in the field of AD research is whether changes that are observed in late-stage AD patients reflect an early or late event in AD. Mild cognitive impairment (MCI) typically progresses to AD and, therefore these cases may be regarded as early AD. However, postmortem samples from MCI cases are rare. Therefore, to test whether changes in alternative splicing machinery may occur in early AD, we re-analysed a published expression array data set of nine controls and 22 AD patients of varying disease severity. Using a threshold-independent analysis to allow the discovery of altered gene groups (as in Barbash & Soreq, 2012), we have found that changes in the 'RNA splicing' category are significantly different from controls already at the incipient AD stage (Supporting Information Fig S4). These changes persisted into severe AD and therefore we conclude that altered pre-mRNA splicing is likely an early defect accompanying the cognitive decline in AD.

In addition to the entorhinal cortices, we analysed pre-central gyrus samples from controls and AD patients and found

  

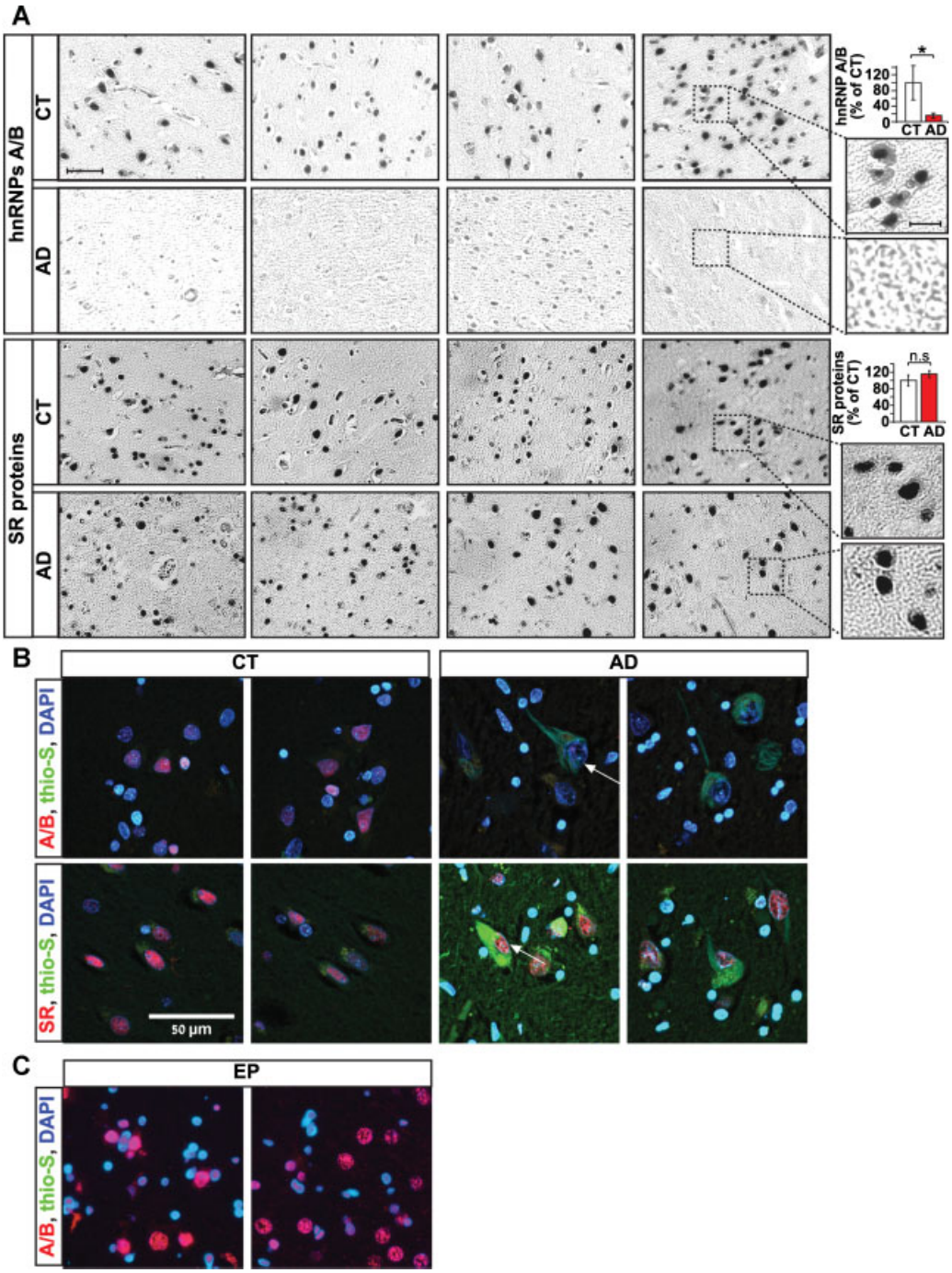


**Figure 2. Selective loss of hnRNP A/B in the entorhinal cortex of AD patients.**

**A.** Immunohistochemistry of hnRNP A/B and SR proteins in human AD and non-demented control entorhinal cortices. Scale bar = 50 μm, in inset = 25 μm. $^{*}p < 0.05$, Student's *t*-test. CT $n = 5$, AD $n = 10$.

**B.** Triple labelling of hnRNP A/B or SR proteins (red), thioflavin-S (plaques and tangles, green) and DAPI (nuclei, blue) demonstrates maintained levels of SR proteins, also in tangled neurons (arrows) and loss of hnRNP A/B in all cells examined. Scale bar 50 μm.

**C.** Comparative hnRNP A/B labelling in the hippocampus of two patients with chronic pharmacoresistant temporal lobe epilepsy (EP). hnRNP A/B (red) and DAPI (blue).

  

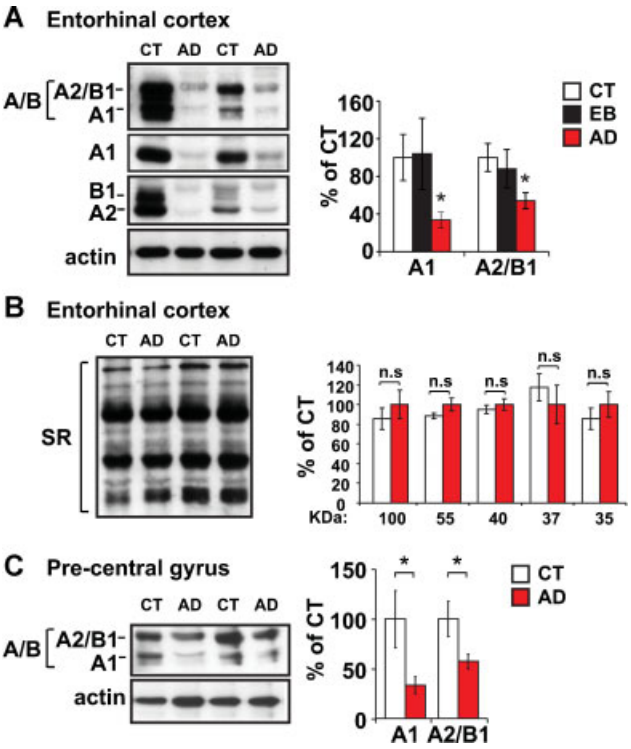


**Figure 3. Immunoblotting corroborates the selective loss of hnRNP A/B in AD.**

**A.** Immunoblotting of the hnRNP A/B family (A/B), hnRNP A1 and A2/B1 in AD and control entorhinal cortex. Columns: densitometric analysis. $^{*}p < 0.05$, one-way ANOVA and Tukey's post-hoc, $n = 12$ for non-demented controls, $n = 9$ for early Braak non-demented controls and $n = 14$ for AD patients.

**B.** Immunoblotting of SR proteins in AD and control entorhinal cortex. Columns: densitometric analysis. n.s., non-significant. Student's *t*-test, $p > 0.05$, $n = 6$ for both groups.

**C.** Immunoblotting of the hnRNP A/B family in AD and control pre-central gyrus. $^{*}p < 0.05$, Student's *t*-test, $n = 8$ for both groups.

significant, albeit less pronounced, reductions in hnRNP A/B levels in this cortical area as well (Fig 3C), suggesting that hnRNP reductions may correlate with brain-region specific damages that occur in AD. Taken together, the different controls used in our analysis suggest that hnRNP A/B loss found in AD is specific for demented patients and is unlikely to be a result of simply diminished number of neurons. To better understand the factors that may contribute we performed both linear and multiple regression analysis. This demonstrated that hnRNP A1 expression is correlated with the AD definition but not age (Supporting Information Table S1) and supported the notion that the extent of hnRNP A/B loss may correlate with disease progression in AD. Additionally, we examined the APP splicing pattern in the AD RNA preparations with hnRNPs depletion. Compatible with others' reports (Matsui et al, 2007), and those reported above, we found preferential inclusion of the APP exon encoding the KPI isoform (Supporting Information Fig S5).

To explore the functional consequences of the hnRNP A/B decline observed in AD we transduced mouse primary mixed cortical cultures with lentivirus particles encoding short-hairpin RNA directed against hnRNP A1 or A2/B1 (here termed shRNA A1 and shRNA A2, respectively). An inert shRNA sequence predicted not to interact with any target in the mouse (shRNAct) served as control. Knocking-down hnRNP A1 did not reduce A2/B1 mRNA levels and *vice versa* (Fig 4A), demonstrating selectivity of the shRNA sequences. Rather, a reduction of hnRNP A1 resulted in a minor (~20%) but significant increase of hnRNP A2/B1, which may suggest a compensatory feedback response. To exclude any residual redundancy, we therefore introduced in all consequent experiments a double knockdown of hnRNP A1 and hnRNP A2/B1 which efficiently reduced the levels of both hnRNP A1 and hnRNP A2/B1 (Fig 4A). Using these experimental tools, we asked if hnRNP A/B reduction *in vivo* impairs learning and memory, the major phenotypic hallmark of AD patients. To this end we used stereotactic injections of shRNA lentivirus to the entorhinal cortex of C57/B6 mice. We first validated the *in vivo* efficiency of viral transduction and the anatomical site of injection using GFP lentivirus. This analysis verified that the entorhinal cortex was faithfully targeted and that the 1 μl of the viral infection (with $6.4 \times 10^8$ ifu/ml) spread into a sphere of 50–70 μm in diameter (Supporting Information Figs S6 and S7). One month following injections we subjected mice injected with the virus particles to sensory-motor tests and found no deficits in their motor activity or visual capabilities (Supporting Information Fig S8). We then tested their learning and memory performance in the Morris water maze, where mice injected with shRNA A1, shRNA A2 and shRNA A1 + A2 lentiviruses showed significantly longer latency to reach a hidden platform than shRNAct injected mice (two-way ANOVA revealed effects of trial number ($F_{11,426} = 2.26$, $p < 0.02$) and treatment ($F_{3,426} = 6.65$, $p < 0.001$). LSD post-hoc comparison: *versus* shA1 $p < 0.01$, shA2 $p < 0.01$, A1 + 2 $p < 0.01$, $n = 10$ in each group, Fig 4B). In a subsequent probe test, when the platform was removed after the training series, shRNA A1, A2 and A1 + A2 injected mice spent a significantly shorter time in the correct quadrant (one-way ANOVA: $F_{3,36} = 9.90$, $p < 0.001$; LSD post-hoc comparison: *vs.* shA1 $^{*}p < 0.01$, shA2 $^{**}p < 0.001$, A1 + 2 $^{**}p < 0.001$; Fig 4C and D). Together, these findings suggest impaired learning and memory capabilities in mice with reduced hnRNP A/B expression in the entorhinal cortex.

In AD patients, electroencephalogram (EEG) abnormalities are repeatedly observed and are hallmarked by slowing of the rhythms and a decrease in coherence among different brain regions, which likely reflect functional disconnections among cortical areas (Jeong, 2004). To further test neuronal network activity, we implanted recording electrodes into the entorhinal cortex of lentivirus-injected mice to record real-time electrocorticography (ECoG) signals throughout the day and night. In all of the tested animals, ECoG analyses revealed clear sleep and wakefulness patterns (Supporting Information Fig S8). Of note, shRNA A1 + A2 knockdown mice showed lower power in the delta (1–2.8 Hz) range when awake ($p < 0.05$, Student's *t*-test), and higher power spectra in the higher 9–12 Hz range during sleep ($p < 0.05$, Student's *t*-test; Fig 4E), suggesting markedly disturbed network activity in the entorhinal cortex of the knockdown mice. In addition to these spectral differences, we

  

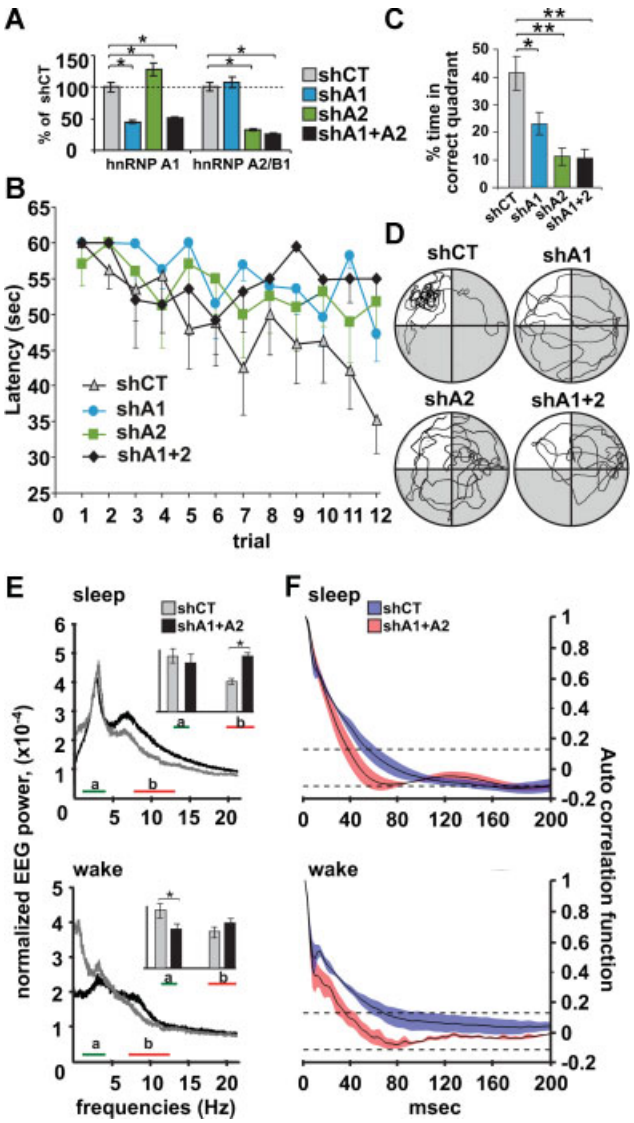


**Figure 4. Knockdown of hnRNP A/B impairs learning and memory and alters cortical network connectivity.**

**A.** Selectivity of lentiviral shRNA-mediated knockdown of hnRNP A1 and/or A2/B1 mRNA in primary cortical cultures. $^{*}p < 0.05$ Student's *t*-test, $n = 6$, performed in duplicates.

**B.** hnRNP A/B knockdown mice show longer escape latencies in the Morris water maze. Two-way ANOVA revealed effects of trial number ($F_{11,426} = 2.26$, $p < 0.02$) and treatment ($F_{3,426} = 6.65$, $p < 0.001$). LSD post-hoc comparison: *versus* shA1 $p < 0.01$, shA2 $p < 0.01$, A1 + 2 $p < 0.01$, $n = 10$ in each group.

**C.** hnRNP A/B knockdown mice spent less time in the correct quadrant in the probe test. One-way ANOVA: $F_{3,36} = 9.90$, $p < 0.001$; LSD post-hoc comparison: *versus* shA1 $^{*}p < 0.01$, shA2 $^{**}p < 0.001$, A1 + 2 $^{**}p < 0.001$.

**D.** Examples of swimming patterns (correct quadrant highlighted).

**E.** ECoG recordings were continuously performed for 4 days from the entorhinal cortex of behaving shA1 + 2 and shCT mice. Fourier transform was performed to derive the power spectrum of each minute, after which all minutes were averaged for each animal in the frequency space. Power spectrums for three mice of each group were averaged and statistically analysed. Representative examples are shown. Bar graph insets are summation of the area below each line for each range. $n = 3$, $^{*}p < 0.05$, Student's *t*-test.

**F.** Autocorrelation patterns of EEG signals. See text for details.

observed a trend for accelerated decay of the autocorrelation patterns of these EEG signals. Autocorrelation analysis searches for correlation of an analysed signal with itself at different time lags, with the correlation being 1 at T0 and gradually decaying with time. In EEG population signals from the hnRNP-knockdown mice, autocorrelation lasted 40 ms on average, whereas in control mice it lasted 80 ms on average ($p = 0.13$, Student's *t*-test) and showed a tendency towards a steeper slope ($p = 0.16$, Student's *t*-test on the power of the exponential function; Fig 4F). These two measures demonstrate a tendency towards faster 'washout time' for the measured EEG signals. Further studies will be required to find out if this trend reflects changes in memory consolidation.

To investigate the cellular and molecular consequences of the hnRNP A/B decline, we tested the effect of lentivirus-shRNA on mature, 14 days in culture neurons. At this time point the expression of synaptic proteins such as synaptophysin is prominent. Given that synapse loss is the best correlate to the cognitive status in AD patients (Armstrong et al, 1991), we focused on this aspect in our analysis. As previously reported in a different system (Patry et al, 2003), hnRNP reduction did not induce overt cell death (Fig 5A and Supporting Information Fig S9). However, immunolabelling of neurons with synaptophysin (a synaptic vesicle marker) and Map2 (a dendritic marker) revealed that suppressing the levels of hnRNP A1, A2/B1 or both in fully matured, 2-week-old cultured primary neurons dramatically reduces dendritic density (Fig 5B). Synaptophysin labelling was reduced (Fig 5C), and puncta were smaller in size (Fig 5E and F). Dendritic density (Fig 5D) and acetylcholinesterase (AChE) activity in the culture medium (Fig 5G) were also reduced in the knockdown neurons, mimicking several hallmarks of AD (Berson et al, 2008). Immunoblots further demonstrated both pre- and post-synaptic deficits in the hnRNP A/B knockdown cultures, reflected in synaptophysin and neuroligin 3 declines (Fig 5H). Importantly, hnRNP A/B knockdown principally recapitulated the alternative splicing events of DRAM2 and Dystonin that were observed in the AD postmortem brain (Fig 5I). To further investigate if hnRNPs A/B can modulate the splicing of transcripts involved in learning and memory we analysed the splicing of exon 19 in the ApoE receptor 2, which is critical for long-term potentiation by Reelin signalling (Beffert et al, 2005). Strikingly, we found that hnRNP A/B knockdown induced the inclusion of E19 in ApoER2 transcripts (Fig 5I), suggesting that hnRNPs A/B loss may also trigger compensatory splicing events in an effort to facilitate LTP, which is drastically reduced by Aβ peptides (Walsh et al, 2002).

To establish whether β-amyloid and tau pathologies affect hnRNP A/B expression *in vivo*, we tested double transgenic APPsw/PS1ΔE9 mice and mice expressing dually mutated K257T/P301S Tau for hnRNP A/B alterations. None of these strains presented such differences (Fig 6A and B). That mutated Tau induces neuronal cell death but does not alter hnRNP A/B

  

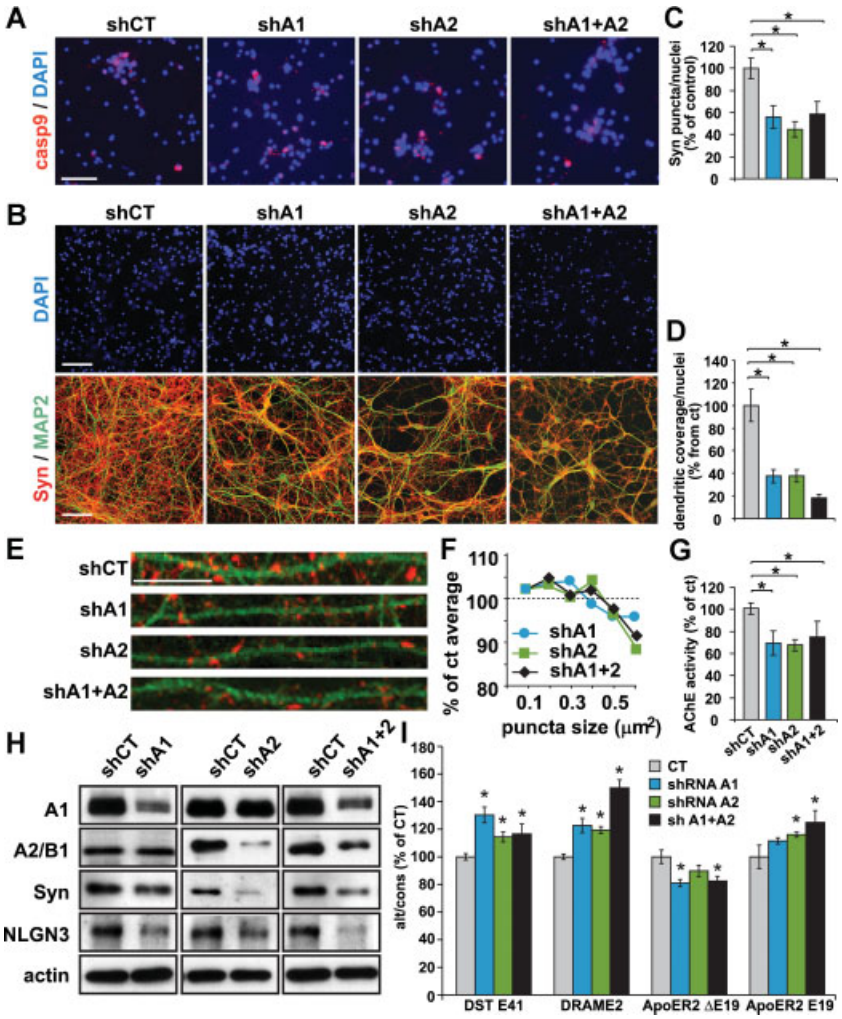


**Figure 5. hnRNP A/B knockdowns in 14 days in culture neurons induce loss of dendrites.**

**A.** No changes in activated caspase 9 (red, see Supporting Information Fig S9 for quantification and other measurements). Scale bar = 50 μm.

**B.** Sustained DAPI staining (top) and reduced dendrites density (green, MAP2, bottom) with reduction of pre-synaptic synaptophysin (pre-synaptic labelling, red, synaptophysin) after hnRNP A/B knockdown in primary cortical neurons. Scale bar = 50 μm.

**C.** Reduced number of puncta stained by synaptophysin in A/B shRNA treated neurons normalized to total nuclei staining. One-way ANOVA: $F_{3,31} = 4.31$, $p < 0.05$; LSD post-hoc: *versus* shA1 $^{*}p < 0.05$, shA2 $^{**}p < 0.01$, A1 + 2 $^{*}p < 0.05$.

**D.** Reduced dendritic density in shRNA A/B treated neurons. One-way ANOVA: $F_{3,32} = 16.21$, $p < 0.001$; LSD post-hoc: *versus* shA1 $^{*}p < 0.001$, shA2 $^{*}p < 0.001$, A1 + 2 $^{*}p < 0.001$.

**E.** Magnified single dendrites and synaptophysin puncta from (**B**) Scale bar = 10 μm.

**F.** Synaptophysin puncta are smaller in shRNA A/B treated neurons. $p < 0.05$ Kolmogorov–Smirnov test.

**G.** Reduced activity of secreted AChE in knockdown cultures. Kruskal–Wallis test: $H_{3,16} = 8.62$, $p < 0.05$. Mann–Whitney *U*-test: *versus* shA1 $^{*}p < 0.05$, shA2 $^{*}p < 0.05$, A1 + 2 $^{*}p < 0.05$.

**H.** Immunoblots of hnRNP A/B, synaptophysin and neuroligin 3 in primary cortical neurons following hnRNP A/B knockdown.

**I.** Alternative splicing of Dystonin, DRAM2 and ApoER2 in mouse primary neurons following hnRNP A/B knockdown has been analysed using Real-time RT-PCR. Alternative exon levels are normalized to a constitutive exon from the same gene. Mann–Whitney *U*-test: *versus* shCT $^{*}p < 0.05$.

expression further supports our findings that these are two disparate phenomena. Moreover, aging did not affect hnRNP A/B expression in either wild-type or transgenic APPsw/PS1ΔE9 mice (Fig 6A). Given that the AD brain is characterized by cholinergic deficits (Bartus et al, 1982), against which anti-cholinesterase therapies are directed (Querfurth & LaFerla, 2010), we subsequently investigated whether cholinergic signalling can regulate neuronal hnRNP A/B levels.

To induce *in vivo* loss-of cholinergic function, we destroyed cholinergic neurons using intra-cerebroventricular (ICV) injections of a saporin-conjugated P75 antibody (muP75-sap) which selectively binds the P75 neurotrophin receptor on the surface of cholinergic neurons, inactivates their ribosomes when penetrating these cells, and causes selective death of cholinergic neurons which leads to learning and memory impairments (Moreau et al, 2008). Entorhinal cortex samples harvested 1 month after muP75-sap injections demonstrated reduced hnRNP A/B expression (Fig 6C), presenting a link between cholinergic cell death and hnRNP A/B loss. SR proteins at large however, were not affected by this cholinergic lesion (Supporting Information Fig S10) providing further support for the selectivity of hnRNP A/B reduction in this model, as well as in the AD brain. To test if this secondary loss in hnRNP A/B causes AD-related alternative splicing aberrations, we re-examined splicing events in CD55, SIPA1L1, Reelin, Dystonin and DRAM2. Strikingly, except for DRAM2, all of these transcripts exhibited increased exon inclusions in the cholinergic deficient mice, similarly to what we observed in the AD brain (Fig 6D). Finally, we induced a gain-of-function effect by incubating primary neuronal cultures with 10 μM of the cholinergic agonist carbachol. Within 48 h, this cholinergic excitation increased the expression of hnRNP A/B (Fig 6E), corroborating the regulation of hnRNP A/B expression by cholinergic signalling and strengthening the notion of causal association between cholinergic deficiencies and the hnRNP depletion in the AD brain.

## DISCUSSION

This study demonstrates previously unforeseen aberrant splicing, reflected by enhanced exon inclusions and accom-

  

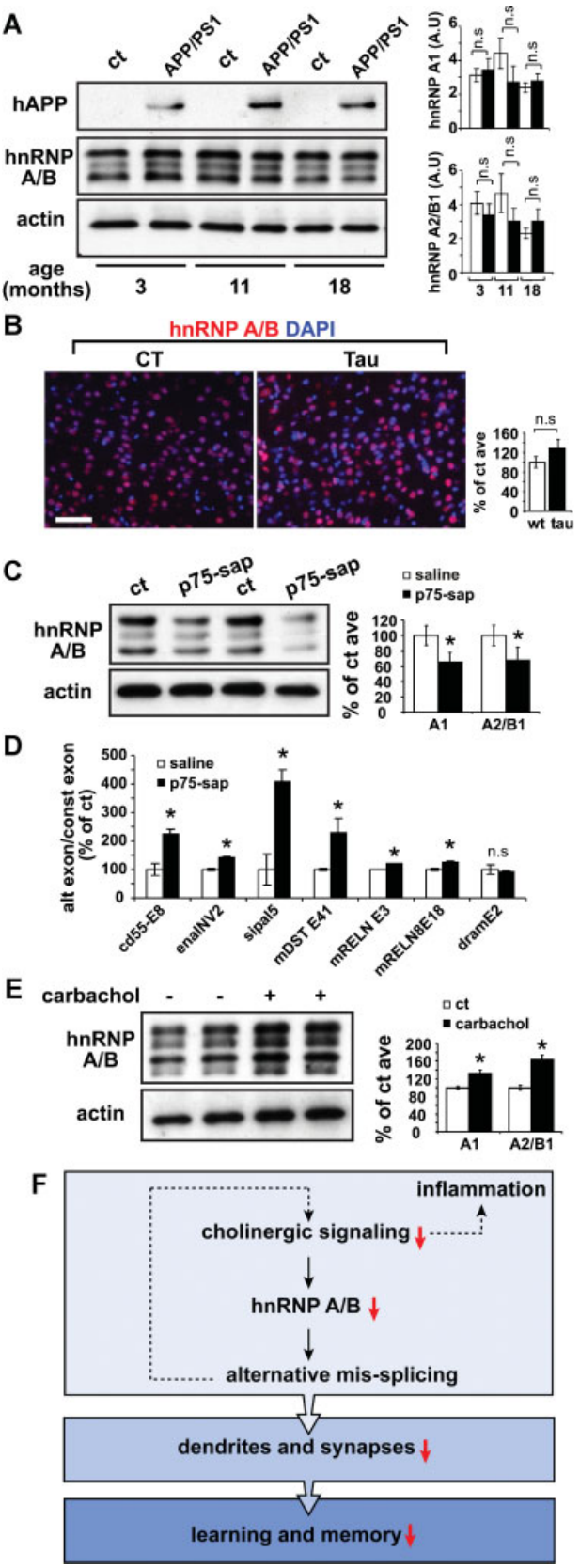


**Figure 6. Mouse hnRNPs A/B levels are modulated by cholinergic signalling but not by Aβ, Tau or aging.**

**A.** hnRNPs A/B levels are similar in APPsw/PS1ΔE9 and non-transgenic siblings in pre- and post-symptomatic mice. $n = 3$ for each group, Mann–Whitney *U*-test: $p$ = NS. Top panel shows expression of human APP.

**B.** Immunofluorescence demonstrates no changes in hnRNPs A/B levels in cortices of double mutated K257T/P301S Tau mice. $n = 6$, $p$ = NS, Student's *t*-test. Scale bar = 50 μm.

**C.** The cholinergic toxin mu p75-sap reduces hnRNPs A/B levels in the entorhinal cortex 1 month following injections. $n \geq 4$, Mann–Whitney *U*-test, $^{*}p < 0.05$.

**D.** Real-time RT-PCR evidence in mu P75-sap injected mice of recapitulated alternative splicing events observed in the entorhinal cortex of AD patients. $n \geq 4$ Mann–Whitney *U*-test, $^{*}p < 0.05$, performed in duplicates.

**E.** hnRNPs A/B are increased in primary neurons following addition of 10 μM of the cholinergic agonist carbachol to the culture medium for 48 h. Student's *t*-test: $n = 6$, $^{*}p < 0.05$.

**F.** Model depicting causes and consequences of hnRNP A/B loss. Reduced cholinergic signalling due to massive death of cholinergic neurons is one of AD hallmarks. Correspondingly, reduced cholinergic input into the entorhinal cortex induces massive loss of hnRNPs A/B expression. Altered cellular levels of hnRNPs A/B induce global splicing impairments including in transcripts that code for proteins with key neuronal functions. This in turn contributes to the loss of synapses and dendrites that negatively affects learning and memory abilities, the key feature of AD.

panied by massive and selective hnRNP A/B loss in AD. In cultured neurons and live mice, we have shown that hnRNP A/B reductions lead to several key features of AD: synapse loss, structural abnormalities of neuronal projections, altered network activity and learning and memory impairments. Several lines of evidence *in vitro* and *in vivo* attribute to the AD-associated impairments in cholinergic signalling a contributing role to hnRNP A/B loss and suggest causal relevance of these impairments to AD.

Our genome-wide analysis identified many disease-related alternative splicing events. While the functional implication of most of these events is currently unknown, we hypothesize that at least part of them may be implicated in the disease process. Recently, genome wide analysis discovered cooperative splicing regulation by different hnRNPs in human cells (Huelga et al, 2012), suggesting that other hnRNPs may also be involved in the context of AD and other neurodegenerative diseases. Importantly, altered ratio between alternatively spliced variants may have dramatic consequences as is evident in frontotemporal dementia, where altered ratio of MAPT transcripts which encode Tau isoforms is key to the disease process.

Alternative splicing of exons can alter critical properties of proteins in the nervous system as is evident in the case of AChE. Inclusion of the extended exon 4 encoding a C-terminal domain which is unique to the 'readthrough' AChE-R variant replaces the otherwise prevalent C-terminus which enables membrane binding of the 'synaptic' AChE-S variant, with functional consequences in stress (Kaufer et al, 1998; Meshorer et al, 2002) and Alzheimer's disease (AD; Berson et al, 2008). As this transcript is expressed in cholinergic brain neurons at 100-fold higher levels than in other neurons (Soreq & Seidman, 2001), such an inclusion is likely to exert functionally important changes on cholinergic neurons. Given that the AChE-R isoform

  

is less stable than AChE-S (Chan et al, 1998), the observed reduction in AChE activity following hnRNP A/B knockdown may arise directly due to a shift in AChE splicing, or alternatively due to indirect mechanisms such as hnRNP A/B control of the expression levels and splicing of many other genes and transcripts (Huelga et al, 2012). Similarly, we cannot overrule the possibility that the reduced levels of neuroligin 3 may have been influenced by alternative splicing of this gene. Alternative splicing plays a major role in controlling the functional properties of the neuroligin family members and has been linked to autism (Yan et al, 2005). Following this line, hnRNP A2 has been shown to be autoregulated in a mechanism involving alternative splicing in its 3′-untranslated region (UTR) that leads to non-sense mediated decay (NMD; McGlincy et al, 2010). Thus, changes in hnRNP A/B expression may lead to altered levels of mRNAs and proteins due to the introduction of premature termination codons or by rendering of the normal stop codon appearing premature.

Suppression of hnRNP A/B due to impaired cholinergic signalling may directly cause key disease hallmarks (Fig 6F). Interestingly, hnRNP A1 over-expression induces alternative splicing of the amyloid precursor protein (APP) mRNA transcript, which is followed by reduced Aβ levels (Donev et al, 2007). This suggests that hnRNP A/B reduction may inversely exacerbate amyloid pathology and thus contribute to the initiation of sporadic AD. Furthermore, hnRNP A1 may be further involved in AD pathogenesis due to its transactivation of the *APOE* promoter activity by direct and specific interaction with a polymorphic site associated with high risk for AD (Campillos et al, 2003; Lambert et al, 2002). Additionally, hnRNP A/B may be involved in other neurodegenerative diseases. Over-expression of hnRNP A2/B1 in a *Drosophila* fragile X-associated tremor/ataxia syndrome (FXTAS) model, rescues the neurodegenerative phenotype caused by multiple CGG repeats in the FMR1 gene (Sofola et al, 2007). This is compatible with the assumption that these repeats bind multiple copies of hnRNP A2/B1, which reduces its effective concentration. Thus, hnRNP A2/B1 reductions cause selective damages to proper neural function both in mammals and in the evolutionarily distant *Drosophila*. RNA metabolism impairments, which are mediated by aberrant hnRNP A/B expression may hence represent a fundamental cause for neural dysfunction and warrant special attention. Strikingly, the very recent identification of a hexanucleotide repeat expansion, which is predicted to bind hnRNP A2/B1, as the cause for chromosome 9p-linked frontotemporal dementia and ALS (DeJesus-Hernandez et al, 2011; Renton et al, 2011) further implicate hnRNP A/B proteins in neurodegeneration.

We note that the observed loss of hnRNP A/B in AD may affect multiple aspects of mRNA metabolism beyond alternative splicing. For example the myelin-basic protein (MBP) mRNA carries a 21-nucleotides long sequence that binds hnRNP A2 (A2RE). This interaction is crucial for the recruitment of MBP mRNA to specific transport granules and for the transport of this mRNA to the periphery of oligodendrocytes (Munro et al, 1999). A2RE is not restricted to glia and has also been found to be encoded by dendritically localized neuronal mRNAs (Shan et al, 2003). Recently, Quaking (Qk) has been found to be a novel regulator of hnRNP A1 mRNA stability. Of note, Qk is involved in myelin formation and is implicated in several disorders including schizophrenia. Moreover, the exons regulated by Qk and hnRNPA1 largely overlap and the gene groups regulated by Qk are most relevant to our current study and include acetylcholine receptor regulators, regulation of synaptic transmission and Tau protein binding (Zearfoss et al, 2011). Future studies should investigate the involvement of these processes in AD.

In conclusion, the loss of hnRNP A/B in AD may have profound implications for our understanding of neurodegenerative disease mechanisms. Furthermore, our results call for a thorough investigation of RNA metabolism impairments in other sporadic neurodegenerative diseases.

## MATERIALS AND METHODS

### Human samples

#### *Neurodegenerative diseases*

Postmortem cortical samples of AD, PD and controls were obtained from The Netherlands Brain Bank (NBB), Netherlands Institute for Neuroscience, Amsterdam. All Material has been collected from donors for or from whom a written informed consent for a brain autopsy and the use of the material and clinical information for research purposes had been obtained by the NBB. Clinical and genotype data for all donors are listed in Supporting Information Table S2.

#### *Epilepsy samples*

Two biopsy specimens were obtained from patients with chronic pharmacoresistant temporal lobe epilepsy who underwent surgical treatment in the Epilepsy Surgery Program at the University of Bonn Medical Center. Presurgical evaluation using a combination of non-invasive and invasive procedures revealed that seizures originated in the mesial temporal lobe in these patients. Surgical removal of the hippocampus was clinically indicated. All procedures were conducted in accordance with the Declaration of Helsinki and approved by the ethics committee of the University of Bonn Medical Center. Informed written consent was obtained from the patients.

### Transgenic mice

APPsw/PS1ΔE9 mice expressing both transgenes under the mouse prion protein promoter were purchased from Jackson Laboratory (Bar Harbor, ME). Mice were maintained as hemizygotes by crossing transgenics to wild-type mice of a B6C3F1/J background. Tail-tip PCR was used for genotyping. Brain sections of Tau mice expressing double mutated K257T/P301S Tau controlled by its natural promoter and age-matched controls were gratefully received from H. Rosenmann (Rosenmann et al, 2008). The joint ethics committee (IACUC) of The Hebrew University and Hadassah Medical Center approved the study protocol for animal welfare (approval #09-12111-4). The Hebrew University is an AAALAC International accredited institute.

### Brain specimens

Mice were anaesthetized by Isoflurane inhalation and decapitated. One hemisphere was transferred to fresh 4% paraformaldehyde in PBS

  

solution immediately after dissection and later embedded in paraffin for histological analysis. The other hemisphere was dissected further, frozen in liquid nitrogen and stored at −70°C for subsequent analyses.

### Primary mixed cortical cultures

Primary mouse cultures of neurons and glia were produced from E16 embryos. Pregnant mice were anaesthetized with isoflurane and sacrificed by cervical dislocation. The uterus was removed and placed on ice. After 5 min the embryo heads were dissected under binocular and cortices were removed, placed in cold DMEM and triturated with a scalpel and up and down pipetting. The medium was replaced with neurobasal medium supplemented with 1:50 B27, 2 mM L-glutamine (Invitrogen, Grand Island, NY), 50 U penicillin and 50 μg/ml streptomycin (Biological Industries, Beit-haemek, Israel), cells were counted and plated in 12 or 24-well plates pre-treated with 10 μg/ml polylysine (Sigma, St. Louis). For confocal microscopy cells were plated on similarly treated glass cover slips. For AChE enzymatic activity and lactate dehydrogenase (LDH) exclusion assay, the cell culture medium was replaced and cells were infected with 1 μl concentrated lentishRNA. The medium was collected 96 h post-infection and stored at −80°C. AChE activity was measured using acetylthiocholine and a 96-well plate modification of the Ellman assay as previously described (Berson et al, 2008). LDH exclusion was also performed in 96-well plate format as described (Berson et al, 2008).

### RNA isolation and RT PCR

Tissues or cells were homogenized in tri reagent (Sigma) and total RNA was extracted as *per* the manufacturer's protocol. RNA concentration was determined with Nanodrop (Thermo, Wilmington, DE) and RNA quality was assessed by gel-electrophoresis. For human samples used in the exon array analysis, RNA quality was determined with Bioanalyzer (Agilent, Santa Clara, CA). RIN values of CT samples: 5.9, 7.4 and 7.1; AD patients: 6.1, 5.9 and 5.6. (Supporting Information Fig S11). These samples were thus validated to include non-degraded RNA sequences. cDNA synthesis (Promega, Madison, WI) involved 0.4 μg RNA samples in 20 μl reactions. Duplicate real-time reverse transcriptase (RT)-PCR tests involved ABI prism 7900HT, SYBR green master mix (Applied Biosystems, Foster City, CA) and ROX, a passive reference dye for signal normalization across the plate. For agarose gel analysis, PCR was performed using Taq DNA polymerase (Sigma). Primer sequences are listed in Supporting Information Table S3. β-actin and GAPDH were used as reference transcripts. Annealing temperature was 60°C for all primers. Serial dilution of samples served to evaluate primers efficiency and the appropriate cDNA concentration that yields linear changes. RT controls verified lack of genomic DNA.

### Western blotting

Tissue samples were kept at −80°C until use. Before homogenization samples were weighed and 800μl (∼×8) cold lysis buffer (0.01 M Tris–HCl pH 7.4, 1 M NaCl, 1 mM EGTA, 1% Triton-X100) containing phosphate inhibitors and protease inhibitors (1:200 of Calbiochem cocktail set III) was added. Samples were lysed with Kontes pellet pestle for the minimal time required, incubated 30 min on ice and centrifuged 30 min at 4°C 17 900 rcf (13 000rpm). Supernatants were transferred to clean test tubes and stored until use at −20°C. Western blots involved standard procedures.

### Immunohistochemistry and immunofluorescence

Paraffin slides were rehydrated by washing in xylene and serial dilutions of ethanol in water. Heat-induced antigen retrieval involved boiling slides in 10 mM pH 6 citrate buffer for 10 min. Hydrogen peroxide methanol quench was performed for slides later developed with 3,3′-diaminobenzidine tetrahydrochloride (DAB). After washing, slides were incubated with 150 μl/slide of blocking buffer (4% normal serum, 0.05% TWEEN20 and 0.3% triton X-100) for 60 min, followed by over-night incubation at 4°C with primary antibody diluted in the blocking buffer. Slides were then washed and incubated with biotin-conjugated secondary antibody for 2 h, after which detection was performed by streptavidin-conjugated Cy (Jackson, West Grove, PA) or by horse raddish peroxidase (HRP) and DAB using the ABC elite kit (Vector, Burlingame, CA). Nuclear staining with 4′,6-diamidino-2-phenylindole (DAPI) was used as counter-staining. Antibodies used include: anti hnRNP A/B (Hua et al, 2008), hnRNP A1, hnRNP A2/B1, tubulin, actin, neuroligin 3 (Santa Cruz, Santa Cruz, CA), activated caspase 9, Synaptophysin, MAP2 (Cell Signaling, Danvers, MA), SR proteins (Invitrogen), human APP (Covance, Emeryville, CA) and GFAP (Sigma). Antibodies dilution: 1:1000 for Western blots, and 1:200 for immunohistochemistry and immunofluorescence.

### Stereotactic injections

Nine-week-old male C57Bl/6J mice were group housed until they underwent stereotaxic surgery, after which they were singly housed throughout all subsequent testing, at a constant temperature (22 ± 1°C) and 12-h light/dark cycles. Mice were anaesthetized by i.p. injections of ketamine (50 mg/kg; Forth Dodge, IA, USA) and domitor (0.5 mg/kg; Orion Pharma, Espoo, Finland) mix, and then mounted in a stereotaxic apparatus for intrahippocampal injections. 0.4 μg/μl mu-P75 SAP (Advanced Targeting Systems, San Diego, CA) was injected intracerebroventricularly (ICV) at the following coordinates (in mm) relative to bregma: AP: −2.0, L: ±1.8, DV: −1.5. Lentiviruses encoding shRNA agents were injected into the entorhinal cortex at: AP: −3.6, L: ±4.8, DV: −4.5. Bilateral injections of 1 μl were conducted using a 10 μl Glenco syringe (Huston, TX, USA). After each injection, the needle was left for 5 min before being slowly retracted to allow complete diffusion.

### Behavioral analysis

#### *Rotarod test*

An accelerating rotarod (Ugo Basile, Comerio VA, Italy) was used for testing motor coordination. The rotarod was set to accelerate from 4 to 40 rpm over 5 min. On the first day, mice were placed on the rotating drum until they did not fall for a period of 30 s. Mice were then tested in three trials with a minimum of 2 min elapsed between trials.

#### *Sensory-motor function tests*

Mice were examined at the peak of their motor activity during the dark phase. Deficits in vestibular function were tested by holding mice by the tail, lifting and then lowering them over a metal cage top. Then, while the mouse was still, a tactile stimulus to the right or left shoulder and trunk was applied using a cotton swab, and orienting to the stimulus was noted. Efficient and symmetric head and limb placement, and symmetric head orienting to tactile stimuli were taken as evidence of normal vestibular functioning.

  

## The paper explained

### PROBLEM:

Recent genetic studies link multiple mutations which impair various steps in RNA metabolism to familial neurodegenerative disease, but the great majority of patients are defined as sporadic, without any known mutation as a cause. We hypothesized that defects in RNA metabolism may also play central roles in non-familial degeneration in Alzheimer's disease (AD), the leading cause of dementia in the elderly.

### RESULTS:

We report that sporadic AD involves acquired changes in RNA metabolism, and more specifically, in alternative splicing. In AD entorhinal cortices, we found globally impaired exon exclusions and selective loss of the hnRNP A/B splicing factors. In primary neurons, hnRNP A/B knockdown induced aberrant splicing and dendrite loss. In mice, this knockdown caused memory impairments and abnormal neural functioning. Interestingly, transgenic mice with disease-associated mutations in APP or Tau, the leading models of AD, displayed no alterations in hnRNP A/B suggesting that its loss in AD is independent of amyloid or Tau toxicity. However, *in vivo* neurotoxin-mediated destruction of cholinergic neurons caused cortical AD-like decrease in hnRNP A/Bs and recapitulated the alternative splicing pattern of AD patients.

### IMPACT:

Our findings uncover hundreds of alternative splicing events that occur in the AD brain and present hnRNP A/B as critical factors for proper neuronal functioning. This work further suggests that preventing RNA metabolism impairments and reinstating normal gene expression patterns may be therapeutically beneficial in AD.

*Water maze test*

The water maze consisted of a round tank, 1.6 m in diameter, filled with water. Mice were trained to find the location of a hidden platform (16 cm in diameter), submerged 1 cm below the water surface, using extra maze visual cues. The training part consisted of four trials per day, with a 1-h break between trials, for 3 days. The escape latency, that is the time required by the mouse to find the platform and climb on it, was recorded for up to 60 s. Each mouse was allowed to remain on the platform for 30 s and was then moved from the maze to its home cage. If the mouse did not find the platform within 60 s, it was placed gently on the platform for 30 s, and then returned to its home cage. On the 4th day of the experiment, the platform was removed and a probe trial was conducted: mice were placed in the maze for 60 s, in which the number of crosses over the four quadrants of the maze was recorded. Increased swimming in the quadrant where the platform was originally placed was considered as an indication of spatial acquisition.

**ECoG**

ECoG recordings were performed using a subcutaneously implanted bipolar transmitter (TA10EA-F20, Data Science International, St. Paul, MN) attached to a pure iridium electrode (WPI, Berlin, Germany) that was perpendicularly inserted in the coordinates described in the EC stereotactic injections (length of the electrode according to the DV coordinate). Reference electrode was placed above the dura through a hole drilled in the skull located 1.5 mm posterior and 1.5 mm lateral to bregma. Both electrodes were affixed with bone-cement (Unifast Trad, GC America, Alsip, IL). Antibiotic treatment (5 mg/kg p.o. enrofloxacin, Bayer, Germany) was given during recovery (7 days). ECoG recordings (at 0.5 or 1 kHz) were performed from 7 days post-operation. All 1 kHz were changed off-line to 0.5 Hz sampling rate. The recording system includes a channel that indicates the quality of the signal for each sample, termed 'activity channel'. Signal fluctuations of the activity channel indicate movements made by the animal as was shown by Zhang et al (Zhang et al, 2007). We used the activity channel output to define the level of motor activity of the animal. Minutes of ECoG recordings were defined as 'sleep epochs' if there was a flat signal in the activity channel, and hence no motor activity of the animal, in the examined minute and 5 min back in time. 'Wakefulness epochs' were defined as minutes where robust fluctuations, above a certain threshold, were visible in activity channel. We next performed Fourier transform to get the power spectrum of each minute and then averaged all minutes for each animal in the frequency space. Power spectrums for three mice of each group were averaged and statistically analysed.

**Exon arrays**

One microgram of total RNA from three non-demented female cotrols and three female AD patients (averge age 73 and 76.5, respectively), was labelled with the Affymetrix exon array whole transcripts sense targeting labelling assay and reagents, including r-RNA reduction and labelling with streptavidin–phycoerithrin. Each sample was hybridized to a GeneChip® Exon 1.0 ST Array (Affymetrix, Santa Clara, CA, USA) according to manufacturer's instructions, and results were scanned to create .CEL files using an Affymetrix GCS 3000 7G scanner and GeneChip Operating Software v. 1.3 to produce .CEL intensity files. Array analysis was performed with Partek Genomic suite (Partek, St. Louis, Missouri) and Altanalyze (Emig et al, 2010). Array data is available from NCBI's Gene expression omnibus (GEO), Series record GSE26972.

**Statistical analysis**

All analysis was done using Prism 5 software. Statistical significance was calculated using Mann–Whitney *U*-test, Student's *t*-test or by one- or two-way ANOVA with LSD post-hoc, where appropriate. Unless otherwise noted, % from control average ± SEM is shown for all graphs.

**Lentivirus-encoded shRNAs**

Active viral particles were produced by co-transfecting Open-Biosystem's TRC pre-cloned shRNA in pLKO.1-Puro vector with

  

plasmids coding for delta R8.2 and VSV-G into HEK-293T cells, using polyethylenimine (Sigma). The packaged virus was collected at 24 and 48 h post-transfection and concentrated using ultracentrifugation (70 000 g, 2 h, 15°C). Dilutions of concentrated virus were followed by infection of HEK-293T cells with diluted virus. The resulting titer was assessed for shRNA expressing viruses using puromycin selection and for GFP expressing viruses counting fluorescing cells (see Supporting Information Figs S3 and S4).

## Author contributions

AB and HS designed the experiments and wrote the paper; AB and GS performed the experiments, with participation of GH; SB analysed microarray and ECoG data and performed lentivirus injections; YG performed qRT-PCR validations of microarray data and immunoblot tests; MK implanted recording electrodes and recorded from behaving animals; AF designed ECoG experiments and advised with analysis of EcoG signals; AJB contributed the epilepsy sections and description; and DSG performed genotype and RT-PCR tests and advised with general aspects of the work.

## Acknowledgements

We thank Drs Rotem Karni and Hanna Rosenmann (Jerusalem) for the pan-hnRNP A/B antibody, K257T/P301S Tau mice tissues and valuable discussions, and Dr Estelle R Bennett, Mr Amit Halberstam (Jerusalem), Ms Raphael Monteran (Paris) and Ms Johanna Wagner (Marbourg) for assistance with experiments. This work was supported by the Legacy Heritage Biomedical Science Partnership Program of the Israel Science Foundation (Grant No. 1799/10), European community's network for Excellence Grant LSH-2004-1.1.5-3, the German Israeli Foundation, the Gatsby and the RoseTrees foundations and the Affymetrix early technological access program (to H. S.). A. B. and G. S. were both supported by Levi Eshkol fellowships.

Supporting Information is available at EMBO Molecular Medicine online

The authors declare that they have no conflict of interest.

## For more information

OMIM:
**http://omim.org/entry/164017O, http://omim.org/entry/600124**

Alzheimer's Disease:
**www.alz.org/, http://www.alzgene.org/, http://www.adni-info.org/**

## References

Armstrong TP, Hansen LA, Salmon DP, Masliah E, Pay M, Kunin JM, Katzman R (1991) Rapidly progressive dementia in a patient with the Lewy body variant of Alzheimer's disease. Neurology 41: 1178-1180

Ashe KH, Zahs KR (2010) Probing the biology of Alzheimer's disease in mice. Neuron 66: 631-645

Barbash S, Soreq H (2012) Threshold-independent meta-analysis of Alzheimer's disease transcriptomes shows progressive changes in hippocampal functions, epigenetics and microRNA regulation. Curr Alzheimer Res 9: 425-435.

Bartus RT, Dean RL, III, Beer B, Lippa AS (1982) The cholinergic hypothesis of geriatric memory dysfunction. Science 217: 408-414

Beffert U, Weeber EJ, Durudas A, Qiu S, Masiulis I, Sweatt JD, Li WP, Adelmann G, Frotscher M, Hammer RE, *et al* (2005) Modulation of synaptic plasticity and memory by Reelin involves differential splicing of the lipoprotein receptor Apoer2. Neuron 47: 567-579

Benmoyal-Segal L, Soreq L, Ben-Shaul Y, Ben-Ari S, Ben-Moshe T, Aviel S, Bergman H, Soreq H (2012) Adaptive alternative splicing correlates with less environmental risk of parkinsonism. Neurodegener Dis 9: 87-98

Berson A, Knobloch M, Hanan M, Diamant S, Sharoni M, Schuppli D, Geyer BC, Ravid R, Mor TS, Nitsch RM, *et al* (2008) Changes in readthrough acetylcholinesterase expression modulate amyloid-beta pathology. Brain 131: 109-119

Burd CG, Dreyfuss G (1994) RNA binding specificity of hnRNP A1: significance of hnRNP A1 high-affinity binding sites in pre-mRNA splicing. EMBO J 13: 1197-1204

Campillos M, Lamas JR, Garcia MA, Bullido MJ, Valdivieso F, Vazquez J (2003) Specific interaction of heterogeneous nuclear ribonucleoprotein A1 with the −219T allelic form modulates APOE promoter activity. Nucleic Acids Res 31: 3063-3070

Chan RY, Adatia FA, Krupa AM, Jasmin BJ (1998) Increased expression of acetylcholinesterase T and R transcripts during hematopoietic differentiation is accompanied by parallel elevations in the levels of their respective molecular forms. J Biol Chem 273: 9727-9733

Chen M, Manley JL (2009) Mechanisms of alternative splicing regulation: insights from molecular and genomics approaches. Nat Rev Mol Cell Biol 10: 741-754

Cooper TA, Wan L, Dreyfuss G (2009) RNA and disease. Cell 136: 777-793

DeJesus-Hernandez M, Mackenzie IR, Boeve BF, Boxer AL, Baker M, Rutherford NJ, Nicholson AM, Finch NA, Flynn H, Adamson J, *et al* (2011) Expanded GGGGCC hexanucleotide repeat in noncoding region of C9ORF72 causes chromosome 9p-linked FTD and ALS. Neuron 72: 245-256

Donev R, Newall A, Thome J, Sheer D (2007) A role for SC35 and hnRNPA1 in the determination of amyloid precursor protein isoforms. Mol Psychiatry 12: 681-690

Du H, Cline MS, Osborne RJ, Tuttle DL, Clark TA, Donohue JP, Hall MP, Shiue L, Swanson MS, Thornton CA, *et al* (2010) Aberrant alternative splicing and extracellular matrix gene expression in mouse models of myotonic dystrophy. Nat Struct Mol Biol 17: 187-193

Emig D, Salomonis N, Baumbach J, Lengauer T, Conklin BR, Albrecht M (2010) AltAnalyze and DomainGraph: analyzing and visualizing exon expression data. Nucleic Acids Res 38: W755-W762

Hua Y, Vickers TA, Okunola HL, Bennett CF, Krainer AR (2008) Antisense masking of an hnRNP A1/A2 intronic splicing silencer corrects SMN2 splicing in transgenic mice. Am J Hum Genet 82: 834-848

Huelga Stephanie C, Vu Anthony Q, Arnold Justin D, Liang Tiffany Y, Liu Patrick P, Yan Bernice Y, Donohue John P, Shiue L, Hoon S, Brenner S, *et al* (2012) Integrative genome-wide analysis reveals cooperative regulation of alternative splicing by hnRNP proteins. Cell Rep 1: 167-178

Jeong J (2004) EEG dynamics in patients with Alzheimer's disease. Clin Neurophysiol 115: 1490-1505

Kabashi E, Valdmanis PN, Dion P, Spiegelman D, McConkey BJ, Vande Velde C, Bouchard JP, Lacomblez L, Pochigaeva K, Salachas F, *et al* (2008) TARDBP mutations in individuals with sporadic and familial amyotrophic lateral sclerosis. Nat Genet 40: 572-574

Kamma H, Portman DS, Dreyfuss G (1995) Cell type-specific expression of hnRNP proteins. Exp Cell Res 221: 187-196

Kashima T, Rao N, David CJ, Manley JL (2007) hnRNP A1 functions with specificity in repression of SMN2 exon 7 splicing. Hum Mol Genet 16: 3149-3159

Kaufer D, Friedman A, Seidman S, Soreq H (1998) Acute stress facilitates long-lasting changes in cholinergic gene expression. Nature 393: 373-377

  

Kocherhans S, Madhusudan A, Doehner J, Breu KS, Nitsch RM, Fritschy JM, Knuesel I (2010) Reduced Reelin expression accelerates amyloid-beta plaque formation and tau pathology in transgenic Alzheimer's disease mice. J Neurosci 30: 9228-9240

Lambert JC, Araria-Goumidi L, Myllykangas L, Ellis C, Wang JC, Bullido MJ, Harris JM, Artiga MJ, Hernandez D, Kwon JM, *et al* (2002) Contribution of APOE promoter polymorphisms to Alzheimer's disease risk. Neurology 59: 59-66

Lefebvre S, Burglen L, Reboullet S, Clermont O, Burlet P, Viollet L, Benichou B, Cruaud C, Millasseau P, Zeviani M, *et al* (1995) Identification and characterization of a spinal muscular atrophy-determining gene. Cell 80: 155-165

Levin MC, Lee SM, Kalume F, Morcos Y, Dohan FC, Jr., Hasty KA, Callaway JC, Zunt J, Desiderio D, Stuart JMC (2002) Autoimmunity due to molecular mimicry as a cause of neurological disease. Nat Med 8: 509-513

Licatalosi DD, Darnell RB (2006) Splicing regulation in neurologic disease. Neuron 52: 93-101

Luo L, O'Leary DD (2005) Axon retraction and degeneration in development and disease. Annu Rev Neurosci 28: 127-156

Matsui T, Ingelsson M, Fukumoto H, Ramasamy K, Kowa H, Frosch MP, Irizarry MC, Hyman BT (2007) Expression of APP pathway mRNAs and proteins in Alzheimer's disease. Brain Res 1161: 116-123

Mayeda A, Krainer AR (1992) Regulation of alternative pre-mRNA splicing by hnRNP A1 and splicing factor SF2. Cell 68: 365-375

McGlincy NJ, Tan LY, Paul N, Zavolan M, Lilley KS, Smith CW (2010) Expression proteomics of UPF1 knockdown in HeLa cells reveals autoregulation of hnRNP A2/B1 mediated by alternative splicing resulting in nonsense-mediated mRNA decay. BMC Genomics 11: 565

Meshorer E, Erb C, Gazit R, Pavlovsky L, Kaufer D, Friedman A, Glick D, Ben-Arie N, Soreq H (2002) Alternative splicing and neuritic mRNA translocation under long-term neuronal hypersensitivity. Science 295: 508-512

Moreau PH, Cosquer B, Jeltsch H, Cassel JC, Mathis C (2008) Neuroanatomical and behavioral effects of a novel version of the cholinergic immunotoxin mu p75-saporin in mice. Hippocampus 18: 610-622

Munro TP, Magee RJ, Kidd GJ, Carson JH, Barbarese E, Smith LM, Smith R (1999) Mutational analysis of a heterogeneous nuclear ribonucleoprotein A2 response element for RNA trafficking. J Biol Chem 274: 34389-34395

Pak DT, Yang S, Rudolph-Correia S, Kim E, Sheng M (2001) Regulation of dendritic spine morphology by SPAR, a PSD-95-associated RapGAP. Neuron 31: 289-303

Park SM, Kim K, Lee EJ, Kim BK, Lee TJ, Seo T, Jang IS, Lee SH, Kim S, Lee JH, *et al* (2009) Reduced expression of DRAM2/TMEM77 in tumor cells interferes with cell death. Biochem Biophys Res Commun 390: 1340-1344

Pastorino L, Sun A, Lu PJ, Zhou XZ, Balastik M, Finn G, Wulf G, Lim J, Li SH, Li X, *et al* (2006) The prolyl isomerase Pin1 regulates amyloid precursor protein processing and amyloid-beta production. Nature 440: 528-534

Patry C, Bouchard L, Labrecque P, Gendron D, Lemieux B, Toutant J, Lapointe E, Wellinger R, Chabot B (2003) Small interfering RNA-mediated reduction in heterogeneous nuclear ribonucleoparticule A1/A2 proteins induces apoptosis in human cancer cells but not in normal mortal cell lines. Cancer Res 63: 7679-7688

Pimplikar SW, Nixon RA, Robakis NK, Shen J, Tsai LH (2010) Amyloid-independent mechanisms in Alzheimer's disease pathogenesis. J Neurosci 30: 14946-14954

Querfurth HW, LaFerla FM (2010) Alzheimer's disease. N Engl J Med 362: 329-344

Renton AE, Majounie E, Waite A, Simon-Sanchez J, Rollinson S, Gibbs JR, Schymick JC, Laaksovirta H, van Swieten JC, Myllykangas L, *et al* (2011) A hexanucleotide repeat expansion in C9ORF72 is the cause of chromosome 9p21-linked ALS-FTD. Neuron 72: 257-268

Rosenmann H, Grigoriadis N, Eldar-Levy H, Avital A, Rozenstein L, Touloumi O, Behar L, Ben-Hur T, Avraham Y, Berry E, *et al* (2008) A novel transgenic mouse expressing double mutant tau driven by its natural promoter exhibits tauopathy characteristics. Exp Neurol 212: 71-84

Shan J, Munro TP, Barbarese E, Carson JH, Smith R (2003) A molecular mechanism for mRNA trafficking in neuronal dendrites. J Neurosci 23: 8859-8866

Sofola OA, Jin P, Qin Y, Duan R, Liu H, de Haro M, Nelson DL, Botas J (2007) RNA-binding proteins hnRNP A2/B1 and CUGBP1 suppress fragile X CGG premutation repeat-induced neurodegeneration in a *Drosophila* model of FXTAS. Neuron 55: 565-571

Sonnenberg A, Liem RK (2007) Plakins in development and disease. Exp Cell Res 313: 2189-2203

Soreq H, Seidman S (2001) Acetylcholinesterase – new roles for an old actor. Nat Rev Neurosci 2: 294-302

Soreq L, Ben-Shaul Y, Israel Z, Bergman H, Soreq H (2012) Meta-analysis of genetic and environmental Parkinson's disease models reveals a common role of mitochondrial protection pathways. Neurobiol Dis 45: 1018-1030

Sreedharan J, Blair IP, Tripathi VB, Hu X, Vance C, Rogelj B, Ackerley S, Durnall JC, Williams KL, Buratti E, *et al* (2008) TDP-43 mutations in familial and sporadic amyotrophic lateral sclerosis. Science 319: 1668-1672

Tai HC, Schuman EM (2008) Ubiquitin, the proteasome and protein degradation in neuronal function and dysfunction. Nat Rev Neurosci 9: 826-838

Uehara T, Nakamura T, Yao D, Shi ZQ, Gu Z, Ma Y, Masliah E, Nomura Y, Lipton SA (2006) S-nitrosylated protein-disulphide isomerase links protein misfolding to neurodegeneration. Nature 441: 513-517

Vance C, Rogelj B, Hortobagyi T, De Vos KJ, Nishimura AL, Sreedharan J, Hu X, Smith B, Ruddy D, Wright P, *et al* (2009) Mutations in FUS, an RNA processing protein, cause familial amyotrophic lateral sclerosis type 6. Science 323: 1208-1211

Villa C, Fenoglio C, De Riz M, Clerici F, Marcone A, Benussi L, Ghidoni R, Gallone S, Cortini F, Serpente M, *et al* (2011) Role of hnRNP-A1 and miR-590-3p in neuronal death: genetics and expression analysis in patients with Alzheimer disease and frontotemporal lobar degeneration. Rejuvenation Res 14: 275-281

Walsh DM, Klyubin I, Fadeeva JV, Cullen WK, Anwyl R, Wolfe MS, Rowan MJ, Selkoe DJ (2002) Naturally secreted oligomers of amyloid beta protein potently inhibit hippocampal long-term potentiation *in vivo*. Nature 416: 535-539

Wang Y, Li Y, Dalle Lucca SL, Simovic M, Tsokos GC Dalle Lucca JJ (2010) Decay accelerating factor (CD55) protects neuronal cells from chemical hypoxia-induced injury. J Neuroinflammation 7: 24

Yan J, Oliveira G, Coutinho A, Yang C, Feng J, Katz C, Sram J, Bockholt A, Jones IR, Craddock N, *et al* (2005) Analysis of the neuroligin 3 and 4 genes in autism and other neuropsychiatric patients. Mol Psychiatry 10: 329-332

Zearfoss NR, Clingman CC, Farley BM, McCoig LM, Ryder SP (2011) Quaking regulates Hnrnpa1 expression through its 3′ UTR in oligodendrocyte precursor cells. PLoS Genet 7: e1001269

Zhang S, Zeitzer JM, Sakurai T, Nishino S, Mignot E (2007) Sleep/wake fragmentation disrupts metabolism in a mouse model of narcolepsy. J Physiol 581: 649-663

Zhang Z, Lotti F, Dittmar K, Younis I, Wan L, Kasim M, Dreyfuss G (2008) SMN deficiency causes tissue-specific perturbations in the repertoire of snRNAs and widespread defects in splicing. Cell 133: 585-600

Zhang C, Frias MA, Mele A, Ruggiu M, Eom T, Marney CB, Wang H, Licatalosi DD, Fak JJ, Darnell RB (2010) Integrative modeling defines the Nova splicing-regulatory network and its combinatorial controls. Science 329: 439-443

  